

Research Article

Development of FRET-Based Assays in the Far-Red Using CdTe Quantum Dots

E. Z. Chong,¹ D. R. Matthews,¹ H. D. Summers,¹ K. L. Njoh,² R. J. Errington,² and P. J. Smith²

¹ School of Physics and Astronomy, Cardiff University, Cardiff, Wales CF24 3AA, UK

² School of Medicine, Cardiff University, Cardiff, Wales CF14 4XN, UK

Correspondence should be addressed to E. Z. Chong, chongez@cf.ac.uk

Received 29 March 2007; Accepted 11 October 2007

Recommended by Marek Osinski

Colloidal quantum dots (QDs) are now commercially available in a biofunctionalized form, and Förster resonance energy transfer (FRET) between bioconjugated dots and fluorophores within the visible range has been observed. We are particularly interested in the far-red region, as from a biological perspective there are benefits in pushing to ~700 nm to minimize optical absorption (ABS) within tissue and to avoid cell autofluorescence. We report on FRET between streptavidin- (STV-) conjugated CdTe quantum dots, Qdot705-STV, with biotinylated DY731-Bio fluorophores in a donor-acceptor assay. We also highlight the changes in DY731-Bio absorptivity during the streptavidin-biotin binding process which can be attributed to the structural reorientation. For fluorescence beyond 700 nm, different alloy compositions are required for the QD core and these changes directly affect the fluorescence decay dynamics producing a marked biexponential decay with a long-lifetime component in excess of 100 nanoseconds. We compare the influence of the two QD relaxation routes upon FRET dynamics in the presence of DY731-Bio.

Copyright © 2007 E. Z. Chong et al. This is an open access article distributed under the Creative Commons Attribution License, which permits unrestricted use, distribution, and reproduction in any medium, provided the original work is properly cited.

1. INTRODUCTION

Förster (or fluorescence) resonance energy transfer was first explored in the 1920s [1] and is increasingly gaining the attention of multidisciplinary researchers. FRET is a technique widely used in probing the conformational changes of biomolecules, examining the structural constitution of a targeted cell and monitoring intracellular processes and many other *in vivo* biological applications [2]. The main attraction of FRET is its sensitivity to very small spatial changes, typically in the nanometer range.

FRET is based on the near field interaction between two molecules (dipoles) in very close proximity, at a distance much smaller than the fluorescence wavelength [3, 4]. The excited state energy of the donor molecule can be transferred to the acceptor molecule in the ground state if there is a considerable overlap between the donor emission and the acceptor absorption. In the past, a variety of organic fluorescent labels were used as probes in FRET measurements [3–5]. However, photobleaching effects have impaired their function as reliable fluorescent markers especially in single-molecule spectroscopic applications. With the discovery of new robust fluorescent material such as semiconduc-

tor quantum dots, the possibility of photobleaching the inorganic markers over extended excitation is no longer an issue. QDs are well known for their photostability, high quantum yield (QY), broad absorption spectrum, and narrow emission spectrum [6–8]. In contrast to the standard organic dyes, these favourable features provide a new route to optically pump different size QDs using the same photoexcitation energy, thus promoting multicolour microscopic imaging. The specific application area which we seek to address is *in vitro* cell cycle and cell lineage studies. In this context we have confirmed that there is no discernible toxic effect of core/shell QDs on the cells over typical analysis period of 1–5 days which corroborates the fact that the release of free ions from the core lattice is largely obviated by the surface passivation [9]. Furthermore, with the advent of the commercial core-shell QDs, a variety of emissions that cover the visible and the infrared spectra are readily available. Therefore, in view of the superior photostability, the biocompatibility and the wide selection of commercial core/shell QDs, the potential of QDs as fluorescent labels is very promising.

In this work, we explored the potential of far-red CdTe/ZnS core-shell Qdot705 (Invitrogen) as an efficient donor in a FRET assay. From the bioimaging perspective,

this avoids the detection of autofluorescence, allows the usage of red excitation which has greater depth of penetration into targeted tissue, and facilitates multiphoton absorption/excitation. From a material point of view, the compositional change from selenide to telluride in Qdot705 also makes it an interesting experimental test subject. Broader emission/absorption spectra and a fluorescence decay lifetime well in excess of 100 nanoseconds at room temperature were seen. In our QD FRET investigation, biotinylated DY731-Bio fluorophores with an absorption peak at 720 nm were self-assembled onto Qdot705-STVs that emit at 705 nm using a streptavidin-biotin binding mechanism in the similar conjugation route as that in [10, 11]. Due to the strong spectral overlap between Qdot705-STV emission and DY731-Bio absorption, FRET signatures were detected in the steady state and also in the time domain spectroscopic measurements.

2. MATERIALS AND METHODS

2.1. DY731-Bio-STV preparation

1 mg of streptavidin powder (Sigma-Aldrich, Dorset, UK) was dissolved in 100 μL phosphate buffered saline (PBS 0.01 M, pH 7.4) to make $\sim 170 \mu\text{M}$ streptavidin solution. 5 μL of the solution was added to 400 μL of 2.5 μM DY731-Bio to give a loading ratio of 1 with respect to DY731-Bio. As a result, the total biotin binding sites outnumbered DY731-Bio. Hence, only streptavidin bound DY731-Bio were generated. The steady-state absorption profile of DY731-Bio-STV bio-complex was recorded with a UV/Vis/NIR Jasco V570 spectrometer (Tokyo, Japan) for determining DY731-Bio-STV molar extinction coefficient.

2.2. Qdot705-STV and DY731-Bio mixture by titrations

10 μL of 1 μM Qdot705-STV stock (Invitrogen, Calif, USA) was dissolved in 400 μL PBS (pH 7.4) in a 10 mm optical path cell. 2 μL of 30 μM DY731-Bio (MoBiTec, Göttingen, Germany) was first dispensed into the QD solution and then followed by 10 successive titrations of 4 μL DY731-Bio. Steady-state photoluminescence (PL) measurements were taken after each titration using a Varian Cary Eclipse fluorimeter (Palo Alto, Calif, USA). For comparison, identical procedures were repeated for control experiments which involved DY731-Bio without the presence of Qdot705-STV.

2.3. Qdot705-STV-DY731-Bio conjugates preparation

5 separate PBS diluted Qdot705-STV solutions (220 μL , $\sim 90 \text{ nM}$) were mixed with increasing amount (4 μL to 200 μL) of 30 μM DY731-Bio to produce Qdot705-STV-DY731-Bio donor-acceptor assay with different labelling ratios. It is estimated that a Qdot705-STV is chemically coupled to 5–10 streptavidin [12]. As streptavidin is a tetrameric protein, approximately 20–40 biotinylated molecules which include DY731-Bio can be arrayed around a single Qdot705-STV. The samples were left to sit at room temperature for 15 minutes. By ultrafiltration with Microcon YM50 spin column (Millipore, Billerica, Mass, USA), the unbound DY731-

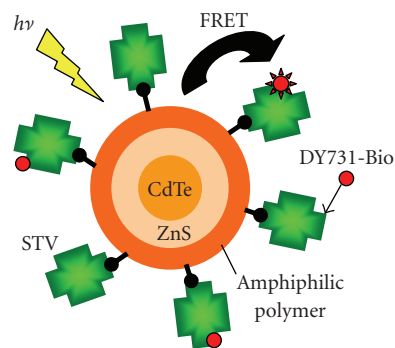


FIGURE 1: Schematic diagram of Qdot705-STV and DY731-Bio in self-assembled assay where energy can be transferred nonradiatively from QD to DY731-Bio upon excitation.

Bio (molecular weight, MW of $\sim 1 \text{ kDa}$) were separated from the conjugated pairs. The column with cutoff MW of 50 kDa was spun at a centrifugal speed of $2000 \times g$ three times for 20 minutes per wash. The collected conjugates were then dissolved in 100 μL PBS in 10 mm path length cuvette for time-resolved PL measurements. The average numbers of DY731-Bio per Qdot705-STV were estimated by steady-state absorption using a UV/Vis/NIR Jasco V570 spectrometer in accordance to the molar extinction coefficient at 663 nm for DY731-Bio-STV.

2.4. Steady-state absorption and photoluminescence measurements

Steady-state absorptions of Qdot705-STV, DY731-Bio, DY731-Bio-STV and Qdot705-STV-DY731-Bio in PBS (pH 7.4) were measured using a UV/Vis/NIR Jasco V570 spectrometer. Ensemble photoluminescence spectra were recorded with a Varian Cary Eclipse fluorimeter. To measure the photoluminescence spectrum of DY731-Bio, 680 nm excitation was chosen. However, the excitation was set to 425 nm for all FRET experiments in order to reduce the direct excitation of DY731-Bio fluorophores. All measurements were performed under ambient conditions.

2.5. Time-resolved photoluminescence measurements

Qdot705-STV-DY731-Bio samples (from Section 2.3) were photoexcited using a Ti:Sapphire laser (Coherent, Santa Clara, Calif, USA) with a repetition rate of 1.1 MHz in order to achieve a longer time window for detecting rather long lived Qdot705-STV photoluminescence. The laser was tuned to 850 nm and was frequency doubled to 425 nm so that direct excitation of DY731-Bio was kept to a minimum. The temporal behaviour of Qdot705-STV in a donor-acceptor assembly was investigated with a Hamamatsu C5680 universal streak camera system (Japan). The photoluminescence of dot ensemble was spectrally filtered using a 700 nm shortpass filter to cutoff unwanted DY731-Bio fluorescence and a 630 nm longpass filter to attenuate any scattered laser. The acquisition of time-resolved photoluminescence was processed using high-performance digital temporal analyser (HPD-TA)

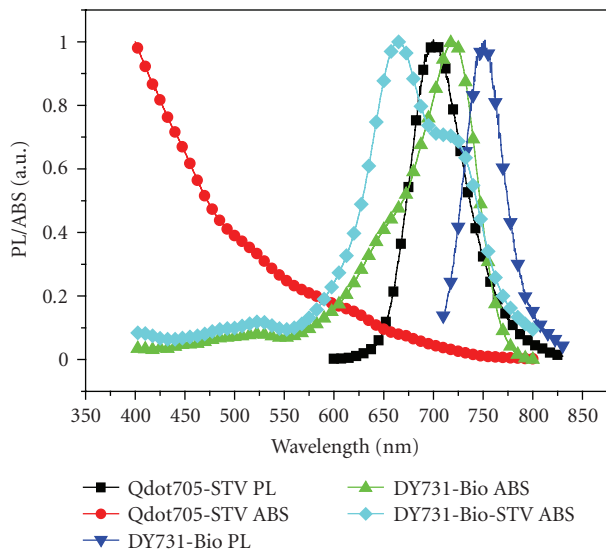


FIGURE 2: Normalised absorption and photoluminescence spectra of Qdot705-STV, DY731-Bio, and DY731-Bio-STV.

software (Hamamatsu, Japan). All measurements were conducted under ambient environmental conditions.

3. RESULTS

3.1. Steady-state spectral measurements

3.1.1. Qdot705-STV and DY731-Bio

As shown in Figure 2, Qdot705-STV sample exhibits a broad, continuous absorption spectrum with no pronounced excitonic peak being resolved. The bulk-like spectrum is due to the relative large size variation in the Qdot705-STV ensemble which have a mean diameter of ~ 20 nm [12]. These QDs fluoresce at 705 nm with a full width at half maximum (FWHM) of 70 nm (-■- in Figure 2). The FWHM of Qdot705-STV emission is approximately 3 times broader than that of the commercial CdSe/ZnS Qdots. The inhomogeneous size distribution is likely to be the reason behind the broad photoluminescence spectrum, however, the crystalline geometry and the lattice defects can also be the cofactors to the line width broadening [13].

Unlike Qdot705-STV, pure DY731-Bio have a narrow absorption spectrum that peaks at 720 nm with a weaker secondary absorption at 660 nm. This strongly coincides with the photoluminescence of Qdot705-STV which spreads across the absorption band of DY731-Bio. However, the absorptivity was modified when DY731-Bio were attached to streptavidin, as depicted in Figure 2. The 660 nm absorption strength rose above that of 720 nm peak. This is possibly due to the conformational changes in bound DY731-Bio molecules. The molar extinction coefficients of DY731-Bio-STV at respective 660 nm and 720 nm were found to be $100\,000\text{ M}^{-1}\text{cm}^{-1}$ and $70\,000\text{ M}^{-1}\text{cm}^{-1}$ instead of $50\,000\text{ M}^{-1}\text{cm}^{-1}$ and $120\,000\text{ M}^{-1}\text{cm}^{-1}$ for pure DY731-Bio.

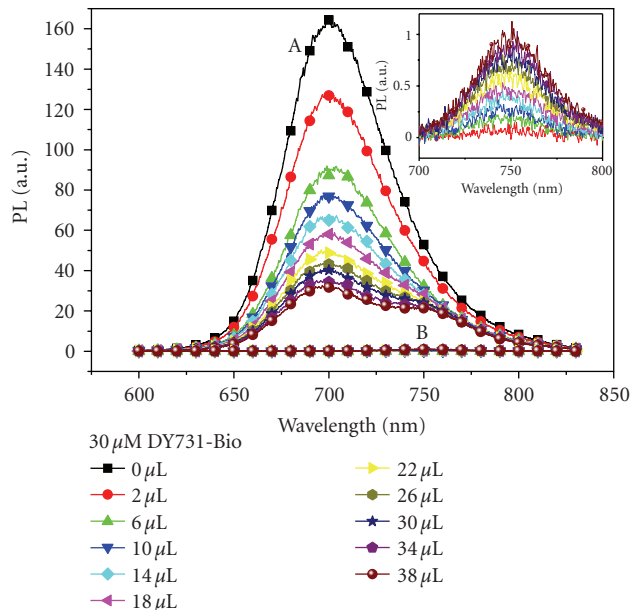


FIGURE 3: Spectra A are the composite photoluminescence of the Qdot705-STV and DY731-Bio mixtures in a series of DY731-Bio titrations. Spectra B are the control photoluminescence of pure DY731-Bio solutions with the equal molar concentration of DY731 as that in the former mixtures. An expanded view of the control spectra is shown in the inset.

The strong overlap between the DY731-Bio absorption and the Qdot705-STV photoluminescence favours the non-radiative energy transfer within the donor-acceptor assay. With the large Stokes shift (~ 30 nm), DY731-Bio are spectrally well separated from Qdot705-STV and hence, the composite photoluminescence spectrum of a mixed donor-acceptor ensemble can be resolved and deconvoluted into respective spectra for further quantitative FRET analysis.

3.1.2. Qdot705-STV and DY731-Bio mixture by titration

Successive titrations with $30\ \mu\text{M}$ DY731-Bio solution resulted in the progressive quenching of Qdot705-STV photoluminescence. Initially, the fluorescence signal at 705 nm dropped abruptly but then gradually levelled off after a total of $\sim 26\ \mu\text{L}$ DY731-Bio have been dispensed into the QD solution. Since the optical densities in the first few titrations ($2\ \mu\text{L}$ - $22\ \mu\text{L}$) were below 0.2, the luminescence quenching in Qdot705-STV was primarily attributed to FRET. The reabsorption of Qdot705-STV photoluminescence by DY731-Bio was anticipated to be less effective. In concomitant with the quenching of Qdot705-STV fluorescence, a systematic enhancement of DY731-Bio photoluminescence was detected as shown in Figure 3(A) with the appearance of a 750 nm peak. The enhanced fluorescence of DY731-Bio in the mixture was many times more intense than the control signal of pure DY731-Bio (see the inset of Figure 3) as the absorption of the solution was dominated by the strong optical interaction with the QD excitons at the excitation wavelength of 425 nm. The quenching of Qdot705-STV emission and the concurrent

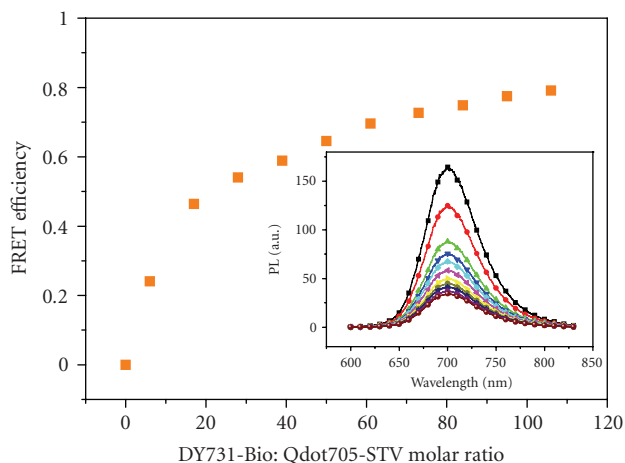


FIGURE 4: The scattered plot represents the FRET efficiency as a function of DY731-Bio to Qdot705-STV molar concentration ratio of nonfiltered mixture. The efficiency calculated is based on the extracted Qdot705-STV spectra (from Spectra A in Figure 3) shown in the inset.

enhancement of DY731-Bio emission signify the occurrence of FRET from the photoexcited Qdot705-STV donors to the ground-state DY731-Bio acceptors.

Since FRET theory is formulated based on proximal dipole-dipole interaction, the excited QDs were generalised as the oscillating dipoles because of the strong electron-hole wavefunction overlap in the core and the weak carrier tunnelling into the wide band gap ZnS shell [14]. FRET efficiency was calculated in accordance to the following equation:

$$E = 1 - \frac{F_{DA}}{F_D}, \quad (1)$$

where F_{DA} is the integrated donor fluorescence in the presence of the acceptor and F_D is the integrated donor fluorescence alone. As the equation is only dependent upon the changes of donor emission intensity with acceptor, the relevant Qdot705-STV spectra were extracted from the composite spectra in Figure 3(A), provided that the spectral shape of Qdot705-STV stayed unchanged throughout the measurements. As depicted in Figure 4, despite the undesirable size, a reasonably high-efficient energy transfer ($\sim 70\%$) can be achieved by Qdot705-STV as the FRET donor since its surface area is large enough to interact with multiple DY731-Bio acceptors. However, the plot of FRET efficiency against acceptor/donor ratio shows some signs of saturation when the molar ratio exceeded 50 : 1. After the 50 : 1 molar ratio, the incremental step in FRET efficiency for successive DY731-Bio titrations scaled down dramatically. Unlike the inorganic QD, the conventional organic dyes are generally confined to single donor-acceptor pairing in a FRET assay because of their comparatively small molecular sizes, which in turn impose strict spatial separation condition between the interacting donor-acceptor molecules (typically less than 100 Å) for achieving high FRET efficiency.

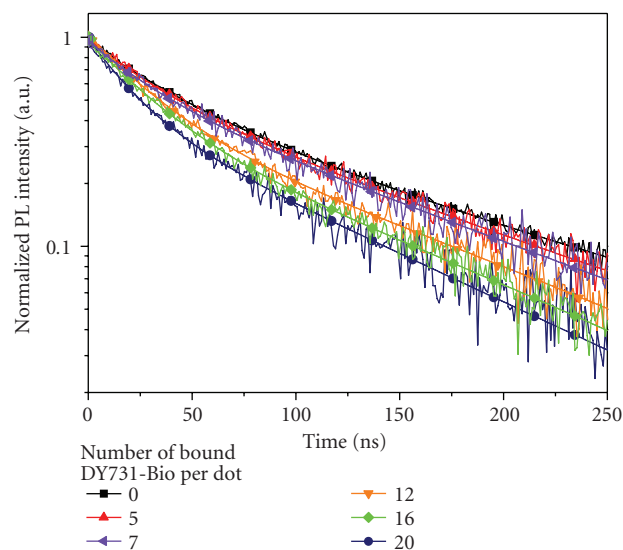


FIGURE 5: Photoluminescence decay of Qdot705-STV with increasing number of labelled DY731-Bio after centrifugation.

3.2. Temporal photoluminescence measurements

3.2.1. Qdot705-STV-DY731-Bio conjugates by ultrafiltration

Due to the partial crosstalk, the Qdot705-STV emission was spectrally separated from DY731-Bio using a 700 nm short-pass filter. By monitoring the temporal changes in the fluorescence spectrum below 700 nm, the interaction dynamics of Qdot705-STV ensembles in the presence of bound acceptors were studied. As illustrated in Figure 5, with increasing number of bound DY731-Bio from 5 to 20 per dot, the QD fluorescence decay was progressively shortened. Henceforth, it would appear that an additional nonradiative relaxation pathway was introduced when DY731-Bio fluorophores were self-assembled around Qdot705-STV: the photoexcited QD excitons recombined at a faster rate by coupling to the radiationless transitions. In view of the fact that a Qdot705-STV can be chemically coupled up to 10 tetrameric streptavidin [12], the highest elicited number of labelled DY731-Bio per QD from the absorption measurement was relatively low compared with the prediction that a maximum 40 biotinylated biomolecules can be possibly assembled around a Qdot705-STV. Therefore, this elucidates, in practise, the average number of streptavidin per QD maybe less than 10, and also the obscuration of some of the binding sites due to the compactness of large streptavidin proteins around the QD is not unlikely.

The fluorescence decay curves shown in Figure 5 depict a complex, multiexponential relaxation of the dots and so a specific method of analysis must be adopted in interpreting the data. We use a biexponential fitting that (i) is the simplest approach outside of a monoexponential model and (ii) provides a conceptual framework for interpretation relating to QD photophysics. There are of course alternative measures that could be adopted, for example, the definition of

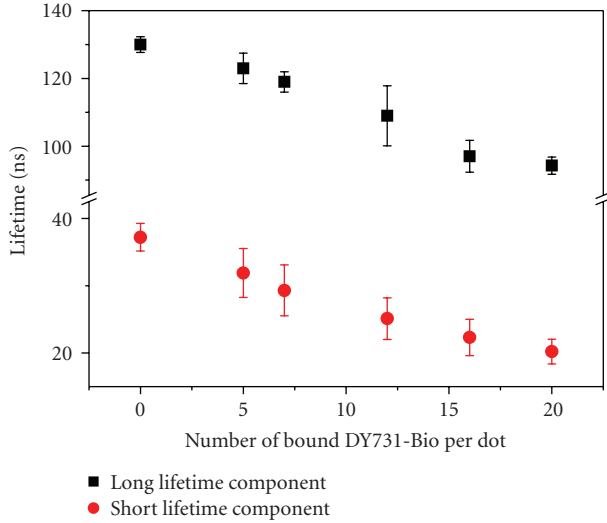


FIGURE 6: Plot of the lifetime components derived from the biexponential fit of Qdot705-STV fluorescence decay versus the number of conjugated DY731-Bio per Qdot705-STV.

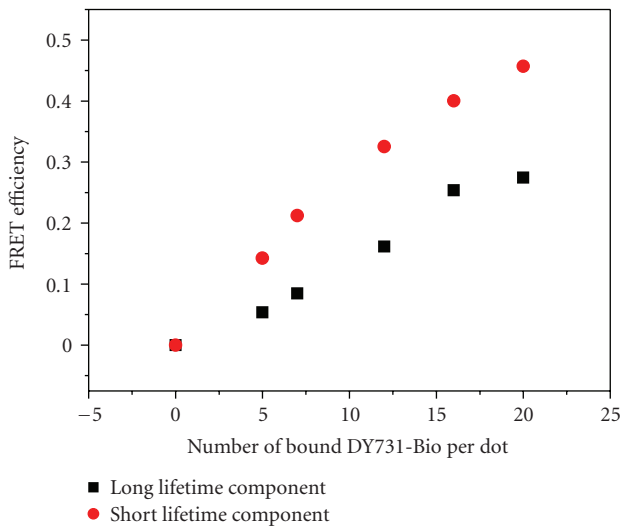


FIGURE 7: FRET efficiency based on Qdot705-STV photoluminescence lifetime measurements plotted against DY731-Bio to Qdot705-STV labelling ratio.

an effective $1/e$ lifetime. Our main purpose in this paper is to highlight the complexity of the QD decay dynamics and assess the ramifications of this in quantifying FRET-based analyses. The fluorescence dynamic of Qdot705-STV was fitted with the decay function:

$$I(t) = A_1 \exp\left(\frac{-t}{\tau_1}\right) + A_2 \exp\left(\frac{-t}{\tau_2}\right) + Z \quad (2)$$

with Z as the baseline. Two distinct lifetime components were derived from the fit. τ_1 fell within 100-nanosecond range and τ_2 fell within 30-nanosecond range. We associate each lifetime component to different, spatially distinct excitonic relaxation paths [15]. From the two lifetime components,

FRET efficiency was explicitly calculated for each dynamic process using the equation below:

$$E = 1 - \frac{\tau_{DA}}{\tau_D}, \quad (3)$$

where τ_{DA} is the donor fluorescence lifetime in the presence of the acceptors and τ_D is the donor fluorescence lifetime without the acceptors. Since FRET is the inverse sixth power to R (donor-acceptor separation), it is intuitive that the efficiency from spatially separated recombination paths will differ. As reflected in Figure 7, the short-lifetime component achieved higher FRET efficiency as compared to that of the long-lifetime component. In this FRET study, we were able to obtain an approximate 46% efficiency from the short-lifetime component at an average 20 bound DY731-Bio per QD. On the contrary, the efficiency was merely 27% for the long-lifetime component at the same labelling ratio. The marked variation asserts the close proximity of the fast decay pathway to the DY731-Bio acceptors.

4. DISCUSSION

Qdot705-STV is a core-shell QD coated with a layer of amphiphilic polymer for water solubility and further surface functionalized with streptavidin for biolinking purposes [16]. Its core is made of direct gap II-VI CdTe with band gap energy of 1.44 eV (at room temperature) [17] which coarsely dictates the emission wavelength of QD. By surface passivation with a larger band gap material like ZnS (3.54 eV at room temperature), the quantum yield of the QDs can be significantly enhanced by suppressing the surface states which may arise from the lattice reconstructions at the final stage of nucleation [6, 7, 18]. However, a perfect passivation is difficult to achieve due to appreciable lattice mismatch between CdTe and ZnS. The lattice constants for CdTe and ZnS are 4.57 Å and 3.81 Å (wurtzite) [17], respectively, which accounts for a total of 17% difference in bond length. In comparison to the visible QDs which are typically made of CdSe, the mismatch is less, at about 12% [6, 19]. So, the surface defects are more predominant in CdTe/ZnS core-shell QDs. The presence of carrier traps near the CdTe/ZnS interface can weaken the oscillator strength of the dipole moment by decreasing the spatial overlap of the exciton wavefunction [20]. Photoexcited electrons are quickly delocalized by surface states, but due to a reduced mobility, the heavier hole is restricted to the inner core. Other factors such as geometrical characteristics of QD (shape and size) can influence the optical absorption as well [13]. Qdot705-STV may not experience the same quantum confinement effects in all dimensions like other commercial visible range Qdots (i.e., Qdot565 and Qdot585) since it adopts a slightly elongated geometry which means that the photoinduced carriers have greater degree of freedom compared to the symmetric spherical QDs [21]. Therefore, the quantization of excited states is less pronounced in the Qdot705-STV absorption spectrum.

Bacterial derivative streptavidin is known to have exceptionally high biotin binding affinity ($K_a \approx 2.5 \times 10^{13} \text{ M}^{-1}$) [22]. Lower nonspecific binding as compared to analogous egg white derivative avidin is an added advantage

in developing superior bioassays for nanosensing devices. In this work, we study the near-field interactions in Qdot705-STV-DY731-Bio self-assembled assay with the use of streptavidin-biotin noncovalent linkers. With the capacity of accommodating multiple bioconjugations and the good spectral overlap between donor emission and acceptor absorption, FRET can occur between large QDs and bioquenchers [23]. In this QD FRET investigation, we were able to achieve high FRET transfer between large Qdot705-STV and DY731-Bio. Besides that, we also observed some drastic changes in the absorption properties of DY731-Bio when they were bound to streptavidin. The 660 nm absorbance was much stronger than the absorbance at 720 nm. The fluorophore probably reoriented itself during the association of streptavidin-biotin and hence, induced some structural changes to accommodate the binding site. It is unlikely that the changes in the absorption were caused by the surface charge of streptavidin since the same spectral shift was detected when DY731-Bio were dispensed in either ethanol or PBS solvents. The analytical interpretation of the FRET-based assay becomes more complicated if the molar extinction coefficient of the acceptor is undesirably modified upon binding. It could possibly influence the overlap integral J , Förster distance R_0 down to the theoretical FRET efficiency prediction.

Strong enhancement in DY731-Bio emission due to radiationless energy transfer from photoexcited Qdot705-STV was observed. Direct excitation at 425 nm was minimal as shown in Figure 3(B). In contrast to the DY731-Bio acceptor, the photoluminescence of Qdot705-STV was quenched drastically during the initial stage of titrations when the majority of the added DY731-Bio should have attached onto QD surface via streptavidin-biotin affinity. Based on the findings in Section 3.2, after the centrifugation with a Microcon filter device, one Qdot705-STV can bind up to 20 biotinylated acceptors. In regard to that information, for a nonfiltered solution, further titrations (between $\sim 20 : 1$ and $\sim 60 : 1$ molar ratio) should only saturate the outermost surface area of the QDs with free DY731-Bio. As a result, the diffused free and the immobilised DY731-Bio were competing for FRET which inherently led to the enhanced efficiency after the molar ratio of $20 : 1$. We speculate that the slow growth in the efficiency after $22 \mu\text{L}$ of DY731-Bio could be the onset of effective radiative quenching by DY731-Bio. It is clear that Qdot705-STV can serve as an efficient donor if the interactions with multiple acceptors are permitted.

The photoluminescence decay of a QD ensemble is multiexponential. The photophysical characteristics in QD ensembles have been correlated to decay-time fluctuations in single QDs [24, 25]. Since the measurements here were taken over an extended period of time, the intensity-dependent effect and the size dispersion in the QD ensemble have averaged out the decay lifetime. The photoluminescence decay can be considered as the collective dynamic behaviour of excited QDs. We statistically fitted the Qdot705-STV photoluminescence decay with discrete biexponential function. The fitted lifetimes were significantly different, 30 nanoseconds and 100 nanoseconds, respectively. Due to a 17% lattice mismatch at the core-shell interface, the formation of fast re-

sponse, carrier trapping states at the surface is highly probable. These surface states provide nonradiative relaxation pathways for the photoinduced electron-hole pairs. Since exciton quenching by surface states usually occurs within subnanosecond times, we attribute the fast decay to carrier trapping by surface states and the slow decay to radiative recombination from the band edge. Besides the QD excitonic state, surface states can also couple to DY731-Bio excited state for radiationless energy transfer provided that the surface-state energy level is within the strong absorption band of DY731-Bio. Instead of taking the amplitude-weighted mean lifetime, FRET generated from two separate transitions were studied independently. From Figure 7, the reduction of the long-lifetime component was less significant than that of the short-lifetime component with increasing conjugation ratio. FRET from surface states was apparently more efficient than that from the band edge level. Assuming that this is due to the R^{-6} relation of FRET, the results are consistent with the interpretation based on the biexponential decay model that the surface states are spatially nearer to labelled DY731-Bio and the band edge recombination primarily occurs within the inner core.

5. CONCLUSIONS

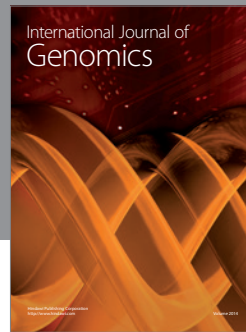
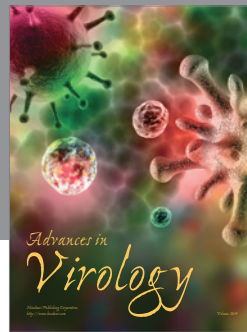
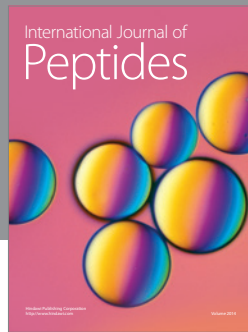
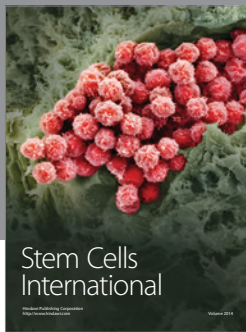
We explored the possibility of FRET in a Qdot705-STV-DY731-Bio assembly with the application of strong streptavidin-biotin binding affinity. By careful selection, we minimized the spectral crosstalk between QD donor and fluorophore acceptor emissions but maximized the spectral overlap between donor emission and acceptor absorption. FRET was derived as the resultant of the quenching effect on QD steady-state fluorescence in stepwise DY731-Bio titrations. An efficiency of $\sim 70\%$ was easily achieved at a molar ratio of 50 acceptors to one QD owing to QD's large surface area. We also recorded the differences in the absorptivity between DY731-Bio and DY731-Bio-STV which could be related to the structural reorientation of fluorophores when molecular complex was formed. However, no further structural studies were conducted to examine the conformation of streptavidin bound DY731-Bio. Any variation in the absorption strength of conjugated acceptor can render FRET less efficient than predicted, if it is based on the optical density of the noninteracting acceptor. By size exclusion filtration, excess DY731-Bio were removed and only Qdot705-STV-DY731-Bio were collected. We achieved ~ 20 acceptors per QD which resulted in $\sim 50\%$ FRET efficiency. Lifetime measurements on the Qdot705-STV-DY731-Bio assay have further confirmed that FRET can be realized despite the undesirable size of QD. However, the highest efficiency obtainable is limited by the number of streptavidin attached to Qdot705-STV.

ACKNOWLEDGMENTS

The authors would like to express their gratitude to EPSRC-GSK for the financial support. E. Z. Chong is funded by GSK under DHPA scheme. They also thank RCUK for the support under the "Optical Biochips" Basic Technology project.

REFERENCES

- [1] R. M. Clegg, "The history of FRET: from conception through the labors of birth," in *Reviews in Fluorescence*, J. R. Lakowicz and C. D. Geddes, Eds., vol. 3, pp. 1–45, Springer, New York, NY, USA, 2006.
- [2] J. R. Lakowicz, *Principles of Fluorescence Spectroscopy*, Springer, Berlin, Germany, 2006.
- [3] I. Z. Steinberg, "Long-range nonradiative transfer of electronic excitation energy in proteins and polypeptides," *Annual Review of Biochemistry*, vol. 40, pp. 83–114, 1971.
- [4] L. Stryer, "Fluorescence energy transfer as a spectroscopic ruler," *Annual Review of Biochemistry*, vol. 47, pp. 819–846, 1978.
- [5] P. G. Wu and L. Brand, "Resonance energy-transfer—methods and applications," *Analytical Biochemistry*, vol. 218, no. 1, pp. 1–13, 1994.
- [6] M. A. Hines and P. Guyot-Sionnest, "Synthesis and characterization of strongly luminescing ZnS-capped CdSe nanocrystals," *Journal of Physical Chemistry*, vol. 100, no. 2, pp. 468–471, 1996.
- [7] B. O. Dabbousi, J. Rodriguez-Viejo, F. V. Mikulec, et al., "(CdSe)ZnS core-shell quantum dots: Synthesis and characterization of a size series of highly luminescent nanocrystals," *Journal of Physical Chemistry B*, vol. 101, no. 46, pp. 9463–9475, 1997.
- [8] X. Peng, M. C. Schlamp, A. V. Kadavanich, and A. P. Alivisatos, "Epitaxial growth of highly luminescent CdSe/CdS core/shell nanocrystals with photostability and electronic accessibility," *Journal of the American Chemical Society*, vol. 119, no. 30, pp. 7019–7029, 1997.
- [9] W. J. Parak, T. Pellegrino, and C. Plank, "Labelling of cells with quantum dots," *Nanotechnology*, vol. 16, no. 2, pp. R9–R25, 2005.
- [10] D. M. Willard, L. L. Carillo, J. Jung, and A. Van Orden, "CdSe-ZnS quantum dots as resonance energy transfer donors in a model protein-protein binding assay," *Nano Letters*, vol. 1, no. 9, pp. 469–474, 2001.
- [11] E. Oh, M. Y. Hong, D. Lee, S. H. Nam, H. C. Yoon, and H. S. Kim, "Inhibition assay of biomolecules based on fluorescence resonance energy transfer (FRET) between quantum dots and gold nanoparticles," *Journal of the American Chemical Society*, vol. 127, no. 10, pp. 3270–3271, 2005.
- [12] Invitrogen, "Qdot streptavidin conjugates user manual," 2006.
- [13] A. P. Alivisatos, "Perspectives on the physical chemistry of semiconductor nanocrystals," *Journal of Physical Chemistry*, vol. 100, no. 31, pp. 13226–13239, 1996.
- [14] A. R. Clapp, I. L. Medintz, and H. Mattoussi, "Förster resonance energy transfer investigations using quantum-dot fluorophores," *ChemPhysChem*, vol. 7, no. 1, pp. 47–57, 2006.
- [15] L. A. Padilha, A. A.-R. Neves, C. L. Cesar, L. C. Barbosa, and C. H. Brito-Cruz, "Recombination processes in CdTe quantum-dot-doped glasses," *Applied Physics Letters*, vol. 85, no. 15, pp. 3256–3258, 2004.
- [16] X. Y. Wu, H. J. Liu, J. Q. Liu, et al., "Immunofluorescent labeling of cancer marker Her2 and other cellular targets with semiconductor quantum dots," *Nature Biotechnology*, vol. 21, no. 1, pp. 41–46, 2003.
- [17] D. R. Lide, Ed., *CRC Handbook of Chemistry and Physics*, CRC Press, Boca Raton, FL, USA, 2001.
- [18] A. P. Alivisatos, "Semiconductor clusters, nanocrystals, and quantum dots," *Science*, vol. 271, no. 5251, pp. 933–937, 1996.
- [19] M. Nirmal and L. Brus, "Luminescence photophysics in semiconductor nanocrystals," *Accounts of Chemical Research*, vol. 32, no. 5, pp. 407–414, 1999.
- [20] Y. Wang and N. Herron, "Nanometer-sized semiconductor clusters: materials synthesis, quantum size effects, and photophysical properties," *Journal of Physical Chemistry*, vol. 95, no. 2, pp. 525–532, 1991.
- [21] B. N.-G. Giepmans, T. J. Deerinck, B. L. Smarr, Y. Z. Jones, and M. H. Ellisman, "Correlated light and electron microscopic imaging of multiple endogenous proteins using Quantum dots," *Nature Methods*, vol. 2, no. 10, pp. 743–749, 2005.
- [22] A. Chilkoti and P. S. Stayton, "Molecular origins of the slow streptavidin-biotin dissociation kinetics," *Journal of the American Chemical Society*, vol. 117, no. 43, pp. 10622–10628, 1995.
- [23] A. R. Clapp, I. L. Medintz, J. M. Mauro, B. R. Fisher, M. G. Bawendi, and H. Mattoussi, "Fluorescence resonance energy transfer between quantum dot donors and dye-labeled protein acceptors," *Journal of the American Chemical Society*, vol. 126, no. 1, pp. 301–310, 2004.
- [24] G. Schlegel, J. Bohnenberger, I. Potapova, and A. Mews, "Fluorescence decay time of single semiconductor nanocrystals," *Physical Review Letters*, vol. 88, no. 13, pp. 1374011–1374014, 2002.
- [25] B. R. Fisher, H.-J. Eisler, N. E. Stott, and M. G. Bawendi, "Emission intensity dependence and single-exponential behavior in single colloidal quantum dot fluorescence lifetimes," *Journal of Physical Chemistry B*, vol. 108, no. 1, pp. 143–148, 2004.



Hindawi

Submit your manuscripts at
<http://www.hindawi.com>

